

Design and Tests of the Hard X-ray Polarimeter X-Calibur

M. Beilicke*, W.R. Binns, J. Buckley, R. Cowsik, P. Dowkontt,
A. Garson, Q. Guo, M.H. Israel, K. Lee, H. Krawczynski
*Department of Physics and McDonnell Center for the Space Sciences,
Washington University in St. Louis, MO, USA (*E-mail: beilicke@physics.wustl.edu)*

M.G. Baring
Rice University, TX, USA

S. Barthelmy, T. Okajima, J. Schnittman, J. Tueller
Goddard Space Flight Center, MD, USA

Y. Haba, H. Kunieda, H. Matsumoto, T. Miyazawa, K. Tamura
Nagoya University, Japan

X-ray polarimetry promises to give new information about high-energy astrophysical sources, such as binary black hole systems, micro-quasars, active galactic nuclei, and gamma-ray bursts. We designed, built and tested a hard X-ray polarimeter *X-Calibur* to be used in the focal plane of the InFOC μ S grazing incidence hard X-ray telescope. X-Calibur combines a low-Z Compton scatterer with a CZT detector assembly to measure the polarization of 10 – 80 keV X-rays making use of the fact that polarized photons Compton scatter preferentially perpendicular to the electric field orientation. X-Calibur achieves a high detection efficiency of order unity.

I. INTRODUCTION

Motivation. Spectro-polarimetric X-ray observations are capable of providing important information to study the non-thermal emission processes of various astrophysical sources – namely the fraction and orientation of linearly polarized photons [1]. So far, only a few missions have successfully measured polarization in the soft (OSO-8 [2]) and hard (Integral [3]) X-ray energy regime. The Crab nebula is the only source for which the polarization of the X-ray emission has been established with a high level of confidence [2, 3]. Integral observations of the X-ray binary Cygnus X-1 indicate a high fraction of polarization in the hard X-ray/gamma-ray bands [4].

Future missions. There are currently no missions in orbit that are capable of making sensitive X-ray polarimetric observations. This will change by the launch of the satellite-borne *Gravity and Extreme Magnetism SMEX* (GEMS) mission [5] scheduled for 2014 (2 – 10 keV). The *Soft Gamma-Ray Imager on ASTRO-H* [6] will also have capabilities of measuring polarization, but the results may be plagued by systematic uncertainties. The hard X-ray polarimeter *X-Calibur* discussed in this paper has the potential to cover the energy range above 10 keV, combining a high detection efficiency with a low level of background and well-controlled systematic errors.

Scientific potential. Synchrotron emission results in linearly polarized photons (electric field oriented perpendicular to the magnetic field lines). The polarized synchrotron photons can be inverse-Compton (IC) scattered by relativistic electrons – weakening the fraction of polarization and imprinting a scattering

angle dependence [7] to the observed fraction of polarization. Other important mechanism for polarizing photons are Thomson scattering and curvature radiation. The scientific potentials of spectro-polarimetric hard X-ray observations are (see Krawczynski et al. (2011) and references therein [1]):

1) *Binary black hole (BH) systems.* Relativistic aberration and beaming, gravitational lensing, and gravitomagnetic frame-dragging will result in an energy-dependent fraction of X-ray polarization from a Newtonian accretion disk [8] since photons with higher energies originate closer to the BH than the lower-energy photons. Schnittman and Krolik [9, 10] calculate the expected polarization signature including the effects of deflection of photons emitted in the disk by the strong gravitational forces in the regions surrounding the black hole and of the re-scattering of these photons by the accretion disk. Spectro-polarimetric observations can constrain the mass and spin of the BH [9], as well as the inclination of the inner accretion disk and the shape of the corona [10].

2) *Pulsars and pulsar wind nebulae.* High-energy particles in pulsar magnetospheres are expected to emit synchrotron and/or curvature radiation which are difficult to distinguish from one another. However, since the orbital planes for accelerating charges that govern these two radiation processes are orthogonal to each other, their polarized emission will exhibit different behavior in position angle and polarization fraction as functions of energy and the phase of the pulsar [3]. In magnetars, the highly-magnetized cousins of pulsars, polarization-dependent resonant Compton up-scattering is a leading candidate for generating the observed hard X-ray tails. In both these classes of neu-

tron stars, phase-dependent spectro-polarimetry can probe the emission mechanism, and provide insights into the magnetospheric locale of the emission region.

3) *Relativistic jets in active galactic nuclei (AGN)*. Relativistic electrons in jets of AGN emit polarized synchrotron radiation at radio/optical wavelengths. The same electron population is believed to produce hard X-rays by inverse-Compton scattering of a photon field. Simultaneous measurements of the polarization angle and the fraction of polarization in the radio to hard X-ray band could help to study (i) synchrotron self-Compton models (X-ray polarization tracks polarization at radio/optical wavelengths in fraction and orientation angle) [7] vs. (ii) external-Compton models for which the hard X-rays will have a relatively small (<10%) fraction of polarization [11]. Polarization also allows one to test the structure (i.e. helical) of the magnetic field of the jet.

4) *Gamma-ray bursts (GRBs)*. GRBs are believed to be connected to hyper-nova explosions and the formation of relativistic jets. As in AGN jets, the structure and particle distribution responsible for GRBs can be revealed by X-ray polarization measurements.

5) *Lorentz invariance*. X-ray polarimetric observations can be used to test theories violating Lorentz invariance [12] with unprecedented accuracies by probing the helicity dependence of the speed of light.

II. DESIGN OF X-CALIBUR

Figure 1 illustrates the conceptual design of the X-Calibur polarimeter. A low-Z scintillator is used as Compton-scatterer. For sufficiently energetic photons, the Compton interaction produces a measurable scintillator signal which is read by a PMT. The scattered X-rays are photo-absorbed in surrounding rings of high-Z Cadmium Zinc Telluride (CZT) detectors. This combination of scatterer/absorber leads to a high fraction of unambiguously detected Compton events. Linearly polarized X-rays will preferably Compton-scatter perpendicular to their E field vector – resulting in a modulation of the azimuthal event distribution.

Each CZT detector ($2 \times 2 \text{ cm}^2$) is contacted with a 64-pixel anode grid and a monolithic cathode facing the scintillator rod. Two detector thicknesses (0.2 cm and 0.5 cm) are being tested in the current setup. Each CZT detector is permanently bonded (anode side) to a ceramic chip carrier which is plugged into the readout board. Figure 2 (left) shows a single CZT detector unit as well as the readout electronics. Each CZT detector is read out by two digitizer boards (32 channel ASIC developed by G. De Geronimo (BNL) and E. Wulf (NRL) [13] and a 12-bit ADC). 16 digitizer boards (8 CZT detectors) are read out by one harvester board transmitting the data to a PC-104 computer. Four CZT detector units form a ring surrounding the scintillator slab. The scintillator EJ-200

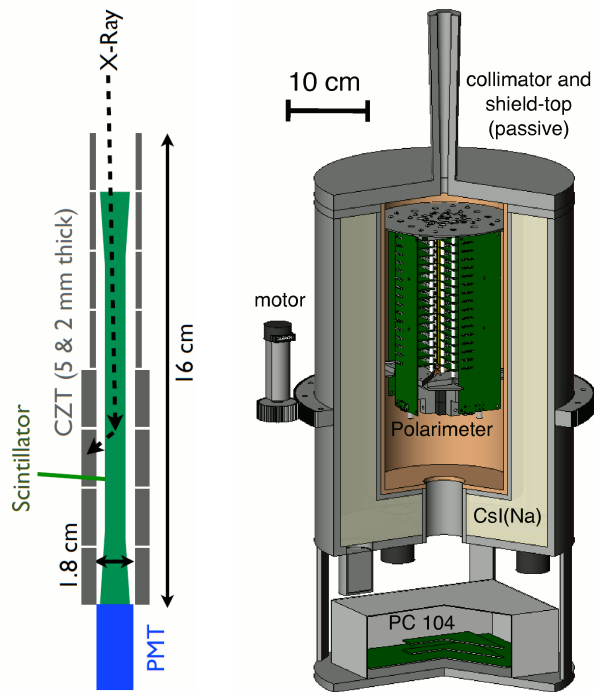


FIG. 1: **Left:** Conceptual design of X-Calibur: Incoming X-rays are Compton-scattered in the scintillator rod (read by a PMT) and are subsequently photo-absorbed in one of the CZT detectors surrounding the rod. **Right:** X-Calibur design with read-out electronics, shielding and azimuthal rotation bearing.

is read by a Hamamatsu R7600U-200 PMT. The PMT trigger information allows to effectively select scintillator/CZT events from the data which represent likely Compton-scattering candidates. The polarimeter and the front-end readout electronics will be located inside an active CsI(Na) anti-coincidence shield with 5 cm thickness and a passive lead shield/collimator at the top (Fig. 1) to suppress charged and neutral particle backgrounds.

We plan to use the X-Calibur polarimeter in the focal plane of the InFOC μ S experiment [14]. A Wolter grazing incidence mirror focuses the X-rays on the X-Calibur polarimeter. In order to reduce the systematic uncertainties (including biases generated by the active shield, a possible pitch of the polarimeter with respect to the X-ray telescope, etc.), the polarimeter and the active shield will be rotated around the optical axis using a ring bearing (see Fig. 1). Counter-rotating masses will be used to cancel the net-angular momentum of the polarimeter assembly during the flight. The advantages of the X-Calibur/InFOC μ S design are (i) a high detection efficiency by using more than 80% of photons impinging on the polarimeter, (ii) low background due to the usage of a focusing optics instead of large detector volumes, and (iii) minimization and control of systematic effects.

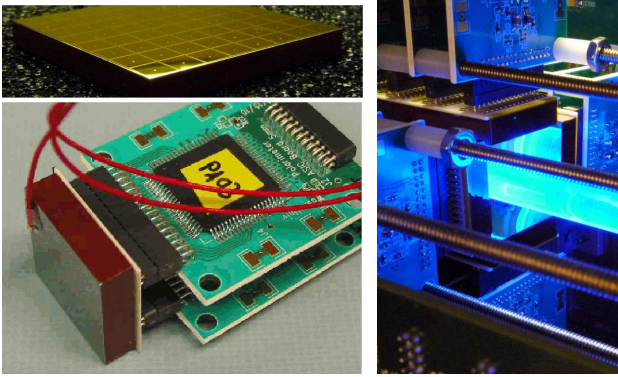


FIG. 2: **Left:** Top: $2 \times 2 \times 0.2 \text{ cm}^3$ CZT detector (64 anode pixels). Bottom: $2 \times 2 \times 0.5 \text{ cm}^3$ detector bonded to a ceramic chip carrier, plugged into 2 ASIC readout boards. The high-voltage cable is glued to the detector cathode (red wire). **Right:** Laboratory version of X-Calibur. The scintillator (blueish glow) is surrounded by two detector rings – each consisting of four 64 pixel CZT detectors.

III. SIMULATIONS

Simulations of the X-Calibur polarimeter were performed using the *Geant4* package [15] with the Livermore low-energy electromagnetic model list. A balloon flight in the focal plane of the InFOC μ S mirror assembly was assumed. We accounted for atmospheric absorption at a floating altitude of 130,000 feet using the NIST XCOM attenuation coefficients [16] and an atmospheric depth of 2.9 g/cm^2 (observations performed at zenith). A Crab-like source was simulated. The X-Calibur modulation factor is $\mu = 0.52$ for a 100% polarized beam. The minimum detectable polarization [1] in the 10–80 keV energy range will be 4% assuming 5.6 hr of on-source observations of a Crab-like source combined with a 1.4 hr background observation of an adjacent empty field. More details about the simulations can be found in Guo et al. (2010) [17].

IV. FIRST MEASUREMENTS

Using funding from Washington University’s McDonnell Center for the Space Sciences, a flight-ready version of the X-Calibur polarimeter was assembled and tested in the laboratory. First measurements were performed with 3 detector rings installed (0.5 cm thickness). Before installation, IV-curves were taken for all detector pixels, followed by a calibration run using a Eu^{152} source (lines at 39.9, 45.7, 121.8 and 344.3 keV). After calibration, a collimated Eu^{152} source was used to determine the azimuthal X-Calibur acceptance for an unpolarized beam. Another data run was taken without a source to determine the background induced by cosmic rays secondaries hitting the detector assembly. Only CZT events with a simulta-

neous ($30 \mu\text{s}$) scintillator trigger are used.

A polarized beam was generated by scattering a strong Cs^{137} source (line at 662 keV) off a lead brick. A lead collimator allowed only X-rays with a scattering angle of $\sim 90 \text{ deg}$ to enter the polarimeter. The X-ray beam of the scattered photons has a mean energy of 288 keV and was polarized to $\sim 55\%$ (modulation factor of $\mu = 0.4$). The expected relative amplitude in the normalized Φ distribution is $0.55 \times 0.4 = 0.22$.

Figure 3 (left) shows the raw spectrum of the first CZT polarimeter ring measured from (i) the polarized beam, (ii) a background spectrum measured without a source and (iii) the excess spectrum corresponding to the energy spectrum of the scattered/polarized beam. As expected, the excess spectrum drops off for energies higher than 288 keV (vertical line) – the energy of the 90 deg-scattered Cs^{137} photons entering the polarimeter. The continuum below this energy is the result of 288 keV photons being Compton-scattered at different depths in the scintillator rod and therefore being reflected to the first CZT ring under different scattering angles and corresponding different Compton energy losses. The little bump in the spectrum around 288 keV may originate from direct CZT hits without a Compton-scattering in the scintillator.

Figure 3 (right) shows the azimuthal scattering distribution of the polarized and unpolarized beam for the second installed CZT detector ring. Only events with a simultaneous scintillator trigger and with a deposited CZT energy between 100 – 330 keV are used (see spectrum in Fig. 3, left). The data of the polarized beam are corrected for the acceptance of the polarimeter (derived from the unpolarized X-ray beam). As expected for a polarized beam, a 180 deg modulation can be seen with a maximum of azimuthal scattering angle perpendicular ($\Phi + 90 \text{ deg}$) to the plane of the E field vector of the polarized beam (indicated by the gray arrows). A sine function was fit to the Φ -distribution of the polarized beam resulting in a relative amplitude of 0.22. The data are in excellent agreement with expectations.

V. SUMMARY AND CONCLUSION

We designed a hard X-ray polarimeter X-Calibur and studied its projected performance and sensitivity for a 1-day balloon flight with the InFOC μ S X-ray telescope. X-Calibur combines a detection efficiency of close to 100% with a high modulation factor of $\mu \approx 0.5$, as well as a good control over systematic effects. X-Calibur was successfully tested/calibrated in the laboratory with a polarized beam of 288 keV photons. We applied for a 1-day X-Calibur/InFOC μ S balloon flight. Our tentative observation program includes galactic sources (Crab, Her X-1, Cyg X-1, GRS 1915, EXO 0331) and one extragalactic source (Mrk 421) for which sensitive polarization measurements would be

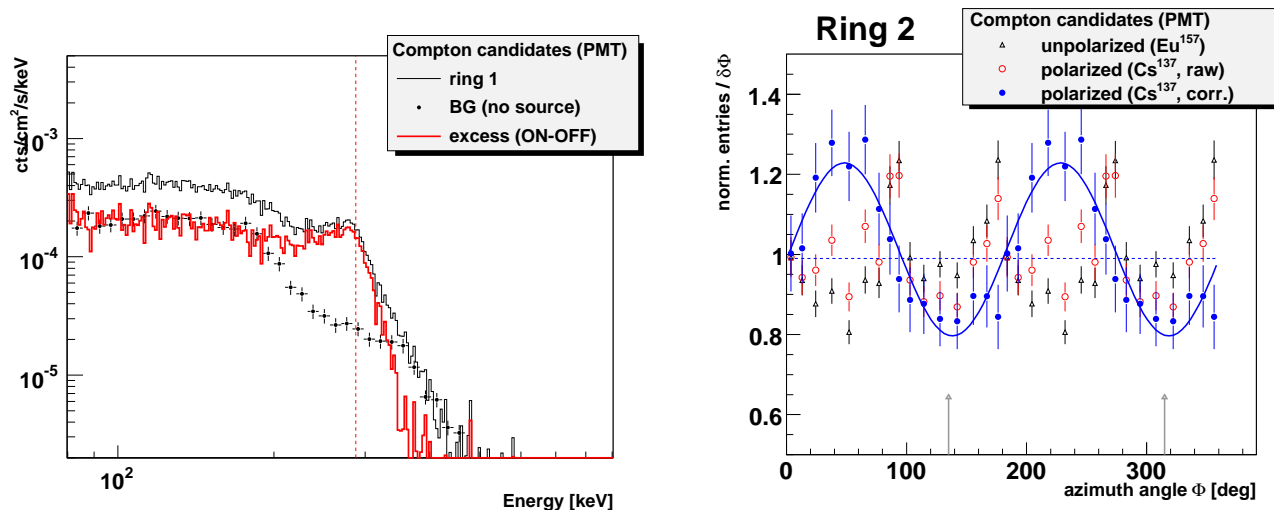


FIG. 3: **Left:** Energy spectrum of 288 keV X-rays (partially polarized) after being scattered in the scintillator (different scattering angles and corresponding energy transfer). The background measurement is done without a source (cosmic rays). The vertical line (288 keV) indicates the energy of the incoming X-ray beam. **Right:** Azimuthal event distribution for the second installed CZT detector ring. Shown are raw events of the polarized beam (red), an unpolarized beam (black), and the acceptance corrected polarized events (blue). A sine function (180deg modulation) was fit to the corrected data of the polarized beam. The vertical arrows indicate the plane of the electric field vector. The 90deg modulation of the unpolarized beam is a result of the 4-fold geometry of the CZT detector assembly.

carried through. We envision follow-up longer duration balloon flights (from the northern and southern hemisphere), possibly using a mirror with increased area. In the ideal case these flights would be performed while the GEMS mission is in orbit to achieve simultaneous coverage in the 0.5–80 keV regime. Successful balloon flights would motivate a satellite-borne hard X-ray polarimetry mission.

Acknowledgments

We are grateful for NASA funding from grant NNX10AJ56G and discretionary funding from the McDonnell Center for the Space Sciences to build the X-Calibur polarimeter. Q.Guo thanks the Chinese Scholarship Council for the financial support (NO.2009629064, stay at Washington University).

-
- [1] H. Krawczynski, et al., “Scientific prospects for hard X-ray polarimetry”, *Aph*, 34 (2011) 550.
 - [2] M. Weisskopf, et al., “Precision measurement of the X-ray polarization of the Crab Nebula without pulsar contamination”, *ApJ*, 220 (1978) L117.
 - [3] A. J. Dean, et al., “Polarized Gamma-Ray Emission from the Crab”, *Science*, 321 (2008) 1183.
 - [4] P. Laurent, et al., “Polarized Gamma-Ray Emission from the Galactic Black Hole Cygnus X-1”, *Science*, 332 (2011) 438.
 - [5] <http://www.cern.ch/accelconf/templates.html>
 - [6] H. Tajima, et al., “Soft gamma-ray detector for the ASTRO-H Mission”, *SPIE*, 7732 (2010) 34.
 - [7] J. Poutanen, “Relativistic jets in blazars: Polarization of radiation”, *ApJS*, 92 (1994) 607.
 - [8] P. A. Connors, & R. F. Stark, “Observable gravitational effects on polarised radiation coming from near a black hole”, *Nature*, 269 (1977) 128.
 - [9] J. D. Schnittman, & J. H. Krolik, “X-ray Polarization from Accreting Black Holes: The Thermal State”, *ApJ*, 701 (2009) 1175.
 - [10] J. D. Schnittman, & J. H. Krolik, “X-ray Polarization from Accreting Black Holes: Coronal Emission”, *ApJ*, 712 (2010) 908.
 - [11] A. L. McNamara, et al., “X-ray polarization in relativistic jets”, *MNRAS*, 395 (2009) 1507.
 - [12] Y.-Z. Fan, et al., “Gamma-ray burst ultraviolet/optical afterglow polarimetry as a probe of quantum gravity”, *MNRAS*, 376 (2007) 1857.
 - [13] E. Wulf, et al., “Compton imager for detection of special nuclear material”, *NIMA*, 579 (2007) 371.
 - [14] Y. Ogasaka, et al., “First light of a hard-x-ray imaging experiment: the InFOCuS balloon flight”, *SPIE*, 5900 (2005) 217.
 - [15] <http://geant4.cern.ch/>
 - [16] <http://www.nist.gov/pml/data/xcom/index.cfm>
 - [17] Q. Guo, et al., “Design of a Hard X-ray Polarimeter: X-Calibur”, arXiv 1101.0595 (2010).